Acta Bot. Croat. 79 (2), 114–120, 2020
DOI: 10.37427/botcro-2020-032

CODEN: ABCRA 25
ISSN 0365-0588
eISSN 1847-8476

Biosynthesis and characterization of iron nanoparticles produced by *Thymus vulgaris* L. and their antimicrobial activity

Ramy Sayed Yehia[1,2], Ali Mohammed Ali[1,3*]

[1] King Faisal University, College of Science, Department of Biological Sciences, Al-Ahsa, 31982 Saudi Arabia
[2] Cairo University, Faculty of Science, Department of Botany and Microbiology, Giza 12613, Egypt
[3] Minia University, Faculty of Science, Department of Botany and Microbiology, El-Minia, 61519, Egypt

Abstract – Research in the area of nanoparticles has grown considerably in recent years. Plant leaf extracts provide a platform for nanoparticle synthesis from metal and metal oxides, which is more economical and environmentally friendly than other methods, such as chemical reduction and physical methods. The present study conducted the biosynthesis of iron nanoparticles (FeNPs) using *Thymus vulgaris* L. (Thyme) leaf aqueous extract. The characterization of FeNPs was carried out by transmission electron microscopy (TEM), UV-visible spectrophotometry (UV-VIS), Fourier transform infrared spectroscopy (FTIR), scanning electron microscopy (SEM) and X-Ray diffraction (XRD) techniques. UV-VIS spectroscopy analysis demonstrated a visible peak around 440 nm. FTIR demonstrated the presence of iron metallic ions. Structural analysis of the nanoparticles by TEM showed agglomerations of spherical shapes. The average size of the synthesized FeNPs was around 40 nm. Regarding application, the ability of the FeNPs to degrade methyl orange was recorded as 95%. They were also examined for potential antimicrobial activity against pathogenic Gram-positive and Gram-negative bacteria and fungi. FeNPs demonstrated high antifungal activity against *Candida albicans*, *C. parapsilosis* and *Aspergillus flavus*, while their antibacterial activity was much weaker compared to commercial antibacterial agent. Thus, FeNPs synthesized using *T. vulgaris* could play an important role in controlling *C. albicans*, *C. parasilosis* and *A. flavus* and bioremediation of dyes.

Keywords: antimicrobial activity, decolorization, methyl orange, nanoparticles, Thymus vulgaris

Introduction

Using chemical and physical methods to produce metal and metal oxide nanomaterials bring with it some challenges because it entails the use of very reactive and toxic reducing agents, which can have undesired impacts on the environment and organisms (Christian et al. 2008). In recent decades, researchers have continuously worked to develop effective, simple, low-cost and reliable green chemistry methods for nanomaterial production. Previous works illustrated that various organisms, such as bacteria (Kianpour et al. 2017), fungi (Yehia and Al-Sheikh 2014), algae (Madhavi et al. 2013), actinomycetes (Ahmad et al. 2015), yeast (Mandal et al. 2006) and higher plants (Herlekar et al. 2014) could act as clean, sustainable and eco-friendly producers for well-functionalized and stable nanomaterials.

Plant extracts have several properties and advantages, including shorter production time, ease of maintaining the cell culture compared with microorganisms (yeast, fungi, bacteria, and algae), so extracting nanomaterials from plants has become increasingly appealing to researchers because plants have unique characteristics, such as high efficiency, eco-friendly products, low cost and nontoxicity (Shah et al. 2015). Several studies illustrated that plant extracts have a high level of antioxidant compounds, such as reducing sugars, nitrogenous bases, reducing agents and amino acids, which can be used as capping and reducing agents in iron or iron oxide nanoparticles (Ebrahiminezhad et al. 2018, Siddiqi et al. 2018, Singh et al. 2018).

Metal nanoparticles, such as iron (Fe), produced through green chemistry are among the most useful materials in nanoscience research (Saif et al. 2016). Various plants have been reported in the green synthesis of iron nanoparticles (FeNPs). For example, FeNPs were synthesized using *Salvia*

* Corresponding author e-mail: ammali@kfu.edu.sa, alimali@mu.edu.eg

officinalis L. (Wang et. al. 2015), *Carica papaya* L. (Latha and Gowri 2014), *Mimosa pudica* L. (Niraimathee et al. 2016), *Passiflora tripartita* Breiter (Kumar et al. 2014), *Hordeum vulgare* L. (Makarov et al., 2014), *Rubus glaucus* Benth. (Kumar et al. 2016), *Andropogon sorghum* (L.) Brot. (Njagi et al. 2011), *Rumex acetosa* L. and *Teucrium polium* L. (Kouhbanani et al. 2019).

The use of NPs in environmental remediation is increasing owing to their ability to decrease costs and improve the efficiency of remediation processes (Zhao et al. 2016). Various nanoparticles have been used successfully for degradation of dye, such as manganese-doped zinc oxide (ZnO), titanium dioxide (TiO_2), cadmium sulphide (CdS), and zinc ferrite ($ZnFe_2O_4$). Nowadays, with the increasing prominence of nanotechnologies, FeNPs and iron oxide nanoparticles (FeONPs) have been studied and used for removing dye contamination (Beheshtkhoo et al. 2018, Kouhbanani et al. 2018).

A member of the family Lamiaceae *Thymus vulgaris* L. is a small perennial therapeutic botanical herb. The plant is a small evergreen shrub that is indigenous to the Mediterranean region but is widely distributed in other parts of the world (Javed et al. 2013). *Thymus vulgaris* extract has many pharmaceutical uses, such as treatment for toothaches, respiratory diseases (bronchitis, asthma, coughing, and whooping coughs), urinary tract infections and dyspepsia. It is also used to prevent hardening of the arteries, increase appetite and expel fungus from stomach because of its important component thymol, which kills bacteria and parasites. In last decades, with the help of the beneficial characters of *T. vulgaris*, different studies have been carried out to demonstrate the pharmacological activities of essential oils and plant extracts (Cowan 1999).

The aim of this work was to prepare well-dispersed FeNPs using an aqueous leaf extract of *T. vulgaris* and to analyse their ability to act as antimicrobial agents against some pathogenic microorganisms. In addition, the ability of the synthesized FeNPs to remove methyl orange was investigated.

Materials and methods

Preparation of leaf extract and FeNPs synthesis

Ferric chloride ($FeCl_3 \cdot 6H_2O$) and methyl orange were purchased from Sigma-Aldrich, USA. All culture media such as nutrient agar and potato dextrose agar (PDA) were purchased from Scharlaus, Spain. All chemicals used in this study were of analytical grade. Solutions were prepared with deionized water. Commercially available dried leaves of *T. vulgaris* were bought from a local market (Al-Hofof, Saudi Arabia). Leaves were washed several times with distilled water to remove dust particles, then dried at room temperature. Leaves were crushed into fine powder with mortar and pestle and finally used for extract preparation. Three grams of dried powdered leaves were added to a flask containing 50 mL of distilled water and then heated at 70 °C with stirring at 600 rpm for 1 h. After cooling to room temperature, the solution was filtered through Whatman filter paper (no. 42). The obtained filtrate was stored at 4 °C overnight. A total of 0.1 M $FeCl_3.6H_2O$ was prepared in double-distilled water (ddH_2O) by dissolving 1.35 g of solid $FeCl_3.6H_2O$ in 50 mL of distilled water. The solution was then mixed with the aqueous leaf extract at a ratio of 1:1 for Fe^{3+} iron reduction. To stimulate the reduction of the Fe^{3+} ions, an equal volume of leaf extract was slowly added to a solution of ferric chloride ($FeCl_3$) and vortexed for 5 min at room temperature. The formation of the FeNPs was confirmed by a change in the colour of solution from light green to black. To purify the FeNPs, centrifugation was carried out at a speed of 5071 *g* and the pellet was washed three times with ethanol and water at a 1:1 ratio, and then dried at 60 °C in an oven.

Physicochemical characterization of FeNPs

UV-VIS absorption analysis was carried out at time intervals of 0, 24, 48 and 72 h using spectrophotometer (Optizen 2120 UV, Mecasys, Korea) in the wavelength range of 300–600 nm. The functional groups prepared in the reaction product were analysed by a Fourier transform infrared spectrophotometer (FTIR) in the wavenumber region (4000–500 cm^{-1}) (PerkinElmer, USA). Samples for transmission electron microscopy (TEM) (JEM-100 CXII transmission electron microscope, JEOL, Japan) were prepared and analysed to determine the shape of the nanoparticles. The size and size distribution of FeNPs were determined by TEM and dynamic light scattering (DLS) analysis by Malvern Zetasizer. X-Ray diffraction (XRD) analysis was used to illustrate the material structure of FeNPs using a Philips X-ray diffraction analyser.

Methyl orange removal assay

To study the photocatalytic activity as FeNPs degrade methyl orange (MO) dye, UV-VIS spectrophotometry was carried out with methyl orange. Briefly, the catalytic activity of FeNPs was estimated by studying the decrease of the methyl orange absorption peak at 465 nm. Then, 20 μg mL^{-1} of FeNPs was added to 10 ml of 25 mg mL^{-1} MO solution and 1 mL of 10% H_2O_2. At different time intervals (0, 15, 30, 60, 120, 180, 240, 300 and 360 min) the concentrations of MO were determined with an Optizen 2120 UV-VIS spectrophotometer (Mecasys) at wavelength 465 nm. Standard curve of known MO concentration was used to determine the decrease in concentration through absorbance. To evaluate the activity of H_2O_2 alone, blank samples were tested without FeNPs. All experiments were performed in triplicate.

Antimicrobial activity of FeNPs

A series of different concentrations of FeNPs was used to measure the antimicrobial activity of FeNPs against bacterial and fungi pathogens. Three pathogenic bacteria (Gram-negative *Escherichia coli* and Gram-positive *Bacillus subtilis* and *Staphylococcus aureus*) and three pathogenic fungi (*Candida albicans*, *C. parapsilosis* and *Aspergillus flavus*) were used in

this experiment. A disc diffusion method was carried out using 10 μg mL^{-1} and 20 μg mL^{-1} concentrations of FeNPs solutions and dilution concentrations with leaf extract (dilution of 10 μg mL^{-1} FeNPs with 10 μg mL^{-1} leaf extract; dilution of 50 μg mL^{-1} leaf extract with 10 μg mL^{-1} FeNPs and dilution of 10 μg mL^{-1} leaf extract with 50 μg mL^{-1} FeNPs). Nutrient agar medium (peptone 5 g L^{-1}, yeast extract 2 g L^{-1}, NaCl 4 g L^{-1}, agar 15 g L^{-1}) was inoculated with freshly prepared cells of each of the above mentioned bacterial species. Sabouraud agar medium (dextrose 40 g L^{-1}, peptone 10 g L^{-1}, agar 15 g L^{-1}) was inoculated with *C. albicans* or *C. parapsilosis*, while potato dextrose agar (PDA) medium (potato extract 4 g L^{-1}, dextrose 20 g L^{-1}, agar 15 g L^{-1}) was inoculated with *A. flavus*. After the agar solidified, several sterilized disks, dipped into FeNPs solutions of the abovementioned concentrations, were placed on the surface of the plates. Disks dipped into 20 μg mL^{-1} solution of commercial antibacterial agent (tetracycline) and antifungal agent (amphotericin) were used as positive controls. The bioactivity of biosynthesized FeNPs was measured as the diameter of the inhibition zone after incubation of the inoculated plates at 37 °C between 24 and 72 h. This experiment was carried out in triplicate.

To examine the effect of nanoparticles on fungi cell morphology, scanning electron microscope (SEM, FEI Company, Hillsboro, OR, USA) samples were prepared as described. Briefly, pure cultures *of C. albicans* and *A. flavus* were fixated for 18 h at 6 °C with 2.5% glutaraldehyde in 0.1 M phosphate buffer (pH 7.2). Then, the samples were washed with 0.1 M phosphate buffer (pH 7.2). Post fixation was performed for 2 h at room temperature with 2% osmium tetroxide. Dehydration was performed in a series of ethanol gradients: 50% and 70% (twice for 10 min), 95% (two times for 5 min) and 100% (two times for 1 min), respectively. Then, samples were dehydrated with acetone (two times for 30 s). Thereafter, the samples were coated with gold and were examined with FEI Quanta 600F Environmental SEM (FEI Company, Hillsboro, OR, USA).

Statistical analysis

All experiments were carried out in triplicate and three independent experiments were also done. Data were illustrated as the mean ± standard deviation (SD). The data were estimated statistically by one-way analysis of variance (ANOVA). For the experiment of the antimicrobial activities Tukey's Multiple Range Test ($P < 0.05$) was carried out as the post-hoc test for mean separations. The differences between values of dye degradation in H_2O_2 alone or combined with FeNPs were analysed using Student's *t*-test.

Results

FeNPs synthesis and characterization

The formation of FeNPs was confirmed by a change in the colour of solution from light green to green or greyish black, which indicates the reduction of iron ions to iron nanoparticles. The colour change was observed within 5–6 h (On-line Suppl. Fig. 1). The results illustrated that a strong surface plasmon resonance (SPR) centred at around 440 nm is characteristic of iron ions. It was found that when iron chloride is added to the plant extract solution, the FeNPs nanoparticles are formed as a result of the exposure to plasma discharge from 24 till 72 h for bacterial and fungal isolates; respectively. The nanoparticles are characterized by the presence of a maximum SPR absorption in the range around 440 nm, which corresponds to iron nanoparticles of mainly spherical shape up to 40 nm in size.

FTIR analysis was carried out to obtain information about the potential biomolecules in the aqueous *T. vulgaris* leaf extract that capped the Fe^{3+}. The IR spectrum of FeNPs is presented in (On-line Suppl. Fig. 1) The IR spectrum of leaf extract showed five major absorption peaks at 3435, 2353, 2083, 1623, and 416 cm^{-1}. Absorption peaks of the signal at 3435 cm^{-1} could be attributed to the O–H stretching vibration of alcohol (–OH) or carboxylic groups (–COOH), and the signal obtained at 2353 cm^{-1} was related to the C–H expansion vibrations of aliphatic acids. The signal observed at 2083 was for $–NH_2$, the signal at 1623 cm^{-1} was attributed to C=O stretched acid or esters, and the signal at 416 cm^{-1} was attributed to C–O stretching.

TEM analysis showed that FeNPs were of spherical shape. The average size ranged around 40 nm (On-line Suppl. Fig 2). The analysis indicated that the size distribution by intensity has two peaks, recorded as 2 nm for peak 1, and around 40 nm for peak 2 (On-line Suppl. Fig. 2).

The results obtained from the XRD analysis are presented in Fig. 1. These results indicate that peaks appearing at 2Θ of 45° showed the presence of zero-valent Fe in the sample. In addition, the analysis showed some low-intensity peaks in between the 2Θ value of 15°, 25°, 32°, 34°, and 38°, indicating that FeNPs surface was coated with FeOOH, organic matter, Fe_3O_4, and Fe_2O_3, respectively.

Removal of methyl orange

The results of removal of MO by FeNPs are illustrated in Fig. 2. The results show that in the absence of FeNPs, no significant removal activity was detected within 360 min.

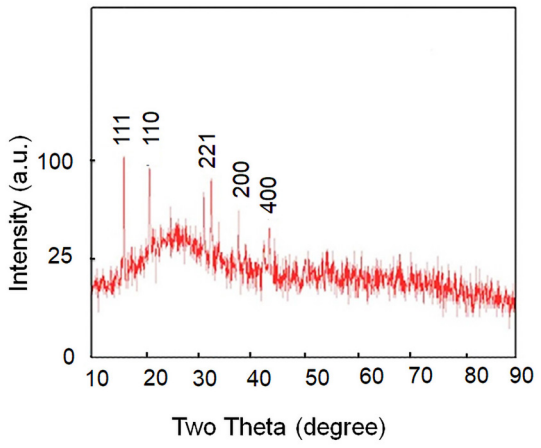

Fig. 1. X-Ray diffraction profiles of FeNPs produced by *Thymus vulgaris* aqueous leaf extract using 10 mL of leaf extract and 0.1 M $FeCl_3 6H_2O$.

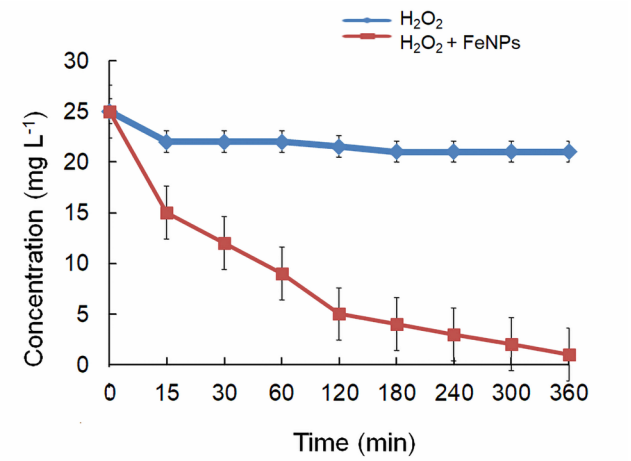

Fig. 2. Diagram of removal of methyl orange (MO) (25 mg mL^{-1}) using 1 mL of 10% H_2O_2 alone or in combination with 20 mg mL^{-1} FeNPs synthesized by *Thymus vulgaris* L. Removal process was presented as reduction in MO concentration.

However, the results illustrated that in the presence of H_2O_2 and 20 μg mL^{-1} FeNPs together, MO concentration reduction occurred rapidly in the initial reaction and afterwards the efficiency of removal significantly increased until 180 min. The efficiency of the decolourization catalysed reaction of the FeNPs was about 95% after 6 h.

FeNPs antimicrobial activity

The diameters of the zones of inhibition (mm) of pathogenic bacteria and fungi treated with FeNPs were shown (On-line Suppl. Fig. 3, On-line Suppl. Tab. 1). The results revealed that the diameters of zones of inhibition, after the addition of 20 μg mL^{-1} FeNPs, were 16 ± 0.12, 15 ± 0.20 and 15 ± 0.19 mm against *B. subtilis*, *S. aureus* and *E. coli* species, respectively, whereas significantly smaller values were obtained after application of 10 μg mL^{-1} FeNPs or dilutions with leaf extract (On-line Suppl. Tab. 1). However, a comparison with the results obtained from the exposure of bacteria to a commercial antibacterial agent (20 μg mL^{-1} tetracycline) revealed that the activity of an equal concentration of FeNPs was significantly less effective than tetracycline.

For the antifungal activity, *C. albicans* and *C. parapsilosis* were found to be more sensitive to FeNPs applied in all concentrations and dilutions with leaf extract than *A. flavus* (On-line Suppl. Fig. 3, On-line Suppl. Tab. 1). Significantly the highest inhibition zone was obtained after the application of 20 μg mL^{-1} FeNPs in all three fungi species, although for *C. albicans* equally high activity was also measured with a dilution of 5 μg mL^{-1} FeNPs and 10 μg mL^{-1} leaf extract. The results obtained for all three fungi species illustrate that the inhibition activity of 20 μg mL^{-1} FeNPs was significantly more effective than the same concentration of the commercial antifungal agent (20 μg mL^{-1} Amphotericin B). For *A. flavus* the dilution of 5 μg mL^{-1} FeNPs and 10 μg mL^{-1} leaf extract exhibited the same effect as 20 μg mL^{-1} Amphotericin, while on *C. albicans* and *C. parapsilosis*, all applied treatments showed better results, except for the 10 μg mL^{-1} FeNPs treatment, which had an effect similar to 20 μg mL^{-1} Amphotericin (On-line Suppl. Tab. 1).

To study the effect of FeNPs on the cell structure of *C. albicans* and *A. flavus*, FeNPs-treated fungi cells were visualized by SEM. Results of the SEM analysis illustrated that upon interaction with the 20 μg mL^{-1} FeNPs, a morphological change in *C. albicans* and *A. flavus* cells appeared as intense damage to the cell membrane, which altered the cell morphology (Fig. 3). The results showed a deformed/squeezed cellular morphology of *C. albicans* (Fig. 3b) compared with control cells (Fig. 3a), which indicates a leakage of the cytoplasmic constituents into the media due to severe membrane damage. FeNPs also initiated severe damage to treated *A. flavus*, resulting in shrunken cells and a distorted cell morphology (Fig. 3d) compared with the control cells (Fig. 3c) The applied FeNPs caused several structural changes in *A. flavus* hyphae, cell wall deformations and local degradation, membrane damage, leading to cytoplasmic leakage and also caused a significant alteration in spore form and germination.

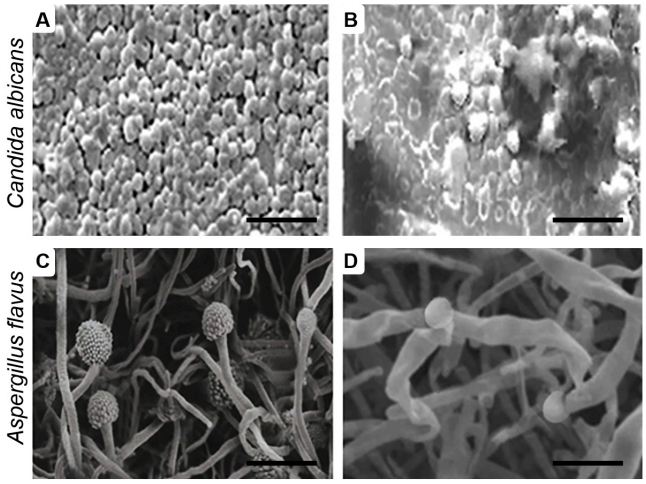

Fig. 3. Scanning electron microscopic images of morphological changes of *Candida albicans* control (A) and treated cell (B), and *Aspergillus flavus* control (C) and treated cell (D). Cells were treated with 20 μg mL^{-1} FeNPs synthesized by *Thymus vulgaris* L. Scale bar is 5 μm.

Discussion

In this study, we reported green synthesis of FeNPs from *Thymus vulgaris* leaves. Many previous studies have explained efficient methods of green synthesis of FeNPs using various plant extracts (Mehdi el al. 2017). Studies on *T. vulgaris* leaf extract indicated the existence of phenolic compounds, especially flavonoids, that featured many of the antioxidant properties in the plant based on their ability to donate hydrogen and a structural requirement considered essential for effective radical scavenging and production of nanoparticles (Takeuchi et al. 2007, Bazylko and Strzelecka 2007, Nasrollahzadeh et al. 2016). *Thymus vulgaris* antioxidants have some unique properties such as being capable of adsorbing onto the nanosurface, reducing the ability to

produce nanoparticles, and determine the size, shape and morphology of the biosynthesized nanoparticles. Furthermore, *T. vulgaris* antioxidants promote the ability of catalysis and prevent the agglomeration process and deformation of the nanosurface (Kulisic et al. 2005). Our results are in agreement with Mehdi et al. (2017), who reported that FeNPs were synthesized within 6 h incubation of the plant extract and $FeCl_3.6H_2O$. A colour change to greyish black indicates the formation of FeNPs over time. The colour changes emerged because of the excitation of the SPR phenomenon of the FeNPs and the optical absorption spectrum of the FeNPs based on their particle size, the surrounding dielectric medium, the shape, and the state of aggregation (Kulkarni et al. 2017).

The green synthesis of FeNPs using *T. vulgaris* was confirmed by UV-VIS spectrophotometry analysis at various times (On-line Suppl. Fig. 1). The results showed a sharp peak at 440 nm, which indicates the formation of FeNPs. Upon addition of the plant aqueous extract into the $FeCl_3.6H_2O$ aqueous solution, the intensity of the peak decreased, indicating the formation of nanoparticles (Khan et al. 2016, Madivoli et al. 2019). These results were compatible with those of other researchers who demonstrated that the SPR peak of FeNPs appeared in the range of approximately 300–500 nm, which is identical to the characteristics of the UV spectral analysis for metallic iron (Kumar et al. 2014, Devatha et al. 2016). The present study results agree with those of Madhavi et al. (2013) who reported that the FeNPs SPR peaks at wavelengths of 402 and 415 nm are attributed to the formation of nanoparticles by brown seaweed (BS, *Sargassum* muticum), and the SPR pattern of metal nanoparticles is related to particle size and the dielectric steady-state of the reaction media and shapes.

The size range of FeNPs synthesized from *T. vulgaris* leaf extract in this study was 40–50 nm. Eslami et al. (2018) and Pattanayak and Nayak (2013) obtained similar results for nanoparticles between 50–100 nm during studies on *Myrtus communis* L., *Thymol* seeds, mango leaves, black tea, green tea leaves, and other plants. The size variety of synthesized nanoparticles results from the inability of secondary metabolites to control particle sizes formed using green approaches. Plant extracts have various secondary metabolites, so they act as stabilizing and reducing agents during the synthesis of metallic nanoparticles. FTIR analysis of the *T. vulgaris* FeNPs in this study showed a similar pattern of absorption bands set in the IR spectra of biosynthetic FeNPs with some degree shift in the band positions. This indicates the possible involvement of flavonoids and other phenolic compounds in the capping of iron ions into FeNPs. These results are in agreement with previous data represented by Luo et al. (2014), who reported that an aqueous extract of *Ageratum conzyoids* L. Asteracese is a mixture of natural organic chemicals, so it is a rich source of capping and reducing agents during FeNPs synthesis.

The removal efficiency of MO dye by FeNPs was about 95% after 6 h. These results revealed that FeNPs synthesized by *T. vulgaris* extract oxidized MO azo dye by a Fenton-like reaction, as mentioned by Trotte et al. (2016). The double bond present in the MO dye works as chromophoric group. Cleavage of this double bond by OH^- leads to MO decolourization (Wang et al. 2014). Previous investigations have illustrated that FeNPs synthesized using various leaf extracts have different capabilities for MO dye removal in liquid environments. In addition, Ebrahiminezhad et al. (2018) illustrated that the removal efficiency of FeNPs synthesized by aqueous extract of Mediterranean cypress for degrading MO was 95.8% after 6 h.

Pathogenic microorganisms are widely spread throughout the world. They have the ability to infect different hosts and to resist antibiotics. Therefore, development of new antimicrobial agents is an urgent need for the treatment and control of these pathogens. Medicinal plants contain a variety of natural compounds that have antimicrobial activity. FeNPs synthesized by plant extract can play a crucial role in improving the therapeutic applicability of plants and can be used as a source of new antimicrobial agents. In the current study, our results illustrated that FeNPs used in the present study caused inhibition in the cell growth of all the tested pathogens, although the efficiency depended on the applied FeNPs concentration alone or in the dilution with leaf extract and on the tested pathogen. The highest FeNPs concentration (20 μg mL^{-1}) applied alone was found to be the most effective for all tested pathogens. Results obtained for growth inhibition of tested bacteria were of moderate success, since a commercial antibacterial agent was more efficient than any of the tested FeNPs concentrations or dilutions with leaf extract. Even more, antibacterial activity was not observed with 10 μg/ml FeNPs against *B. subtilis*. Diao and Yao (2009) illustrated that treatment with nanoparticles reduced *B. subtilis* viability by 80–100%. In contrast, in the present study we found that no reduction in viability with 10 μg mL^{-1} of FeNPs and with an increase of the concentration to 20 μg mL^{-1} *B. subtilis* growth inhibition occurred. This disagreement suggested that size and concentration of nanoparticles may influence the antimicrobial effect, with different species and strains presenting variations in the range of resistance or susceptibility to FeNPs. Lee et al. (2008) reported the inactivation of *E. coli* by zero-valent iron nanoparticles and this inactivation could be due to the penetration of the small particles (10–80 nm) into *E. coli* membranes. Nanoparticles could then react with intracellular oxygen, leading to oxidative stress, eventually causing disruption of the cell membrane. The antifungal activity of *T. vulgaris*-FeNPs against *C. albicans*, *C. parapsilosis*, and *A. flavus* was investigated using antifungal Amphotericin B as a comparable control. Our results showed that FeNPs exhibited a potent antifungal activity against *C. albicans*, *C. parasilosis* and *A. flavus*. Kim el al. (2007) revealed the potent activity of AgNPs against *C. albicans*. Saraniya and Bhimba (2014) also revealed higher antifungal activity of AgNPs against *C. albicans*, *C. parapsilosis*, and *A. niger*. Seddighi et al. (2017) reported the inhibitory effect of FeONPs aganist *C. tropicalis*, *C. albicans* and *C. glabrata*. They reported that the antifungal activity of FeONPs improved as the concentration of the nanopar-

ticles increased. Also, similar results showing that the activity of nanoparticles depends upon concentration were documented by Kim et al. (2007). Hassan et al. (2019) reported the antimicrobial activity of SeNPs against *E. coli*, *S. aureus*, *C. albicans* and *A. flavus*. They illustrated that the inhibitory zone diameter of the tested microorganisms increased as the concentration of SeNPs was increased. Also Violeta et al. (2011) demonstrated that the antimicrobial activity is influenced not only by the concentration but also by the size of the nanoparticles.

In the present study, the normal cell of *C. albicans* and *A. flavus* has a spherical shape. smooth cell wall and intact cell membrane, but when *C. albicans* and *A. flavus* were treated with FeNPs and subjected to SEM, the damage to and rupture of their cell wall were detected. The effect of high concentration of FeNPs on the treated fungi was observed as membrane damage of cells and some pits that have been caused in intracellular components leading to leakage and finally cell death. Jay and Shafkat (2018) proposed that nanoparticles might attach to the surface of the cell membrane disturbing permeability and respiratory function of the cell. In addition, it may be possible that the nanoparticles not only interact with the surface of membrane but can also penetrate inside the microorganisms. The antimicrobial activity of metal nanoparticles may occur in two ways. The first one is the formation of H_2O_2 on nanoparticle`s surface due to the possible formation of a hydrogen bond between hydroxyl groups of cellulose molecules of fungi with oxygen atom of nanoparticles leading to inhibition of the microbial growth, while the second one is the release of metal ions+ that causes damages of cell membrane and interacts with intracellular contents (Moraru et al., 2003). Similarly, several nanoparticles have exhibited strong antimicrobial properties through different mechanisms as photocatalytic production of reactive oxygen species that damage cell components (Violeta el al. 2011).

Acknowledgments

The authors acknowledge the Deanship of Scientific Research at King Faisal University for the financial support under Nasher Track (Grant No. 186213).

References

Ahmad, M.S., Yasser, M.M., Sholkamy, E.N., Ali, M.A., Mehanni, M.M., 2015: Anticancer activity of bio-stabilised selenium nanorods synthesized by *Strepromyces bikiniensis* strain Ess_amA-1. International Journal of Nanomedicine 10, 3389–3401.

Bazylko, A., Strzelecka, H., 2007: A HPTLC densitometric determination of luteolin in *Thymus vulgaris* and its extracts. Fitoterapia 78, 391–395.

Beheshtkhoo, N., Kouhbanani, M.J., Savardashtaki, A., Mani, A.M., Taghizadeh, S., 2018: Green synthesis of iron oxide nanoparticles by aqueous leaf extract of *Daphne mezereum* as a novel dye removing material. Applied Physics A 124, 363.

Christian, P., Von der Kammer, F., Baalousha, M., Hofmann, T., 2008: Nanoparticles: structure, properties, preparation and behavior in environmental media. Ecotoxicology 17, 326–343.

Cowan, M.M., 1999: Plant Products as Antimicrobial Agents. Journal Clinical Microbiology Reviews 12(4), 564–582.

Devatha, H., Thalla, A., Katte, S., 2016: Green synthesis of iron nanoparticles using different leaf extracts for treatment of domestic waste water. Journal of Cleaner Production 139, 1425–1435.

Diao, M., Yao, M., 2009: Use of zero-valent iron nanoparticles in inactivating microbes. Water Research 43, 5243–5251.

Ebrahiminezhad, A., Zare-Hoseinabadi, A., Sarmah, A.K., Taghizadeh, S., Ghasemi, Y., Berenjian, A., 2018: Plant-mediated synthesis and applications of iron nanoparticles. Molecular Biotechnology 60, 154–168.

Eslami, S., Ebrahimzadeh, M.A., Biparva, P., 2018: Green synthesis of safe zero valent iron nanoparticles by *Myrtus communis* leaf extract as an effective agent for reducing excessive iron in iron-overloaded mice, a thalassemia model. RSC Advances 8(46), 26144–26155.

Hassan, A.A., Mogda, K.M., Nahed, M.A.S. Rasha, M.H.S., 2019: Influence of selenium nanoparticles on some bacterial and fungal causes of mastitis in buffaloes. Animal Health Research 7(1), 76–94.

Herlekar, M., Barve, S., Kumar, R., 2014: Plant-mediated green synthesis of iron nanoparticles. Journal of Nanoparticle Research 2014, 1–9.

Javed, H., Erum, S., Tabassum, S, Ameen, F., 2013: An overview on medicinal importance of *Thymus vulgaris*. Journal of Asian Scientific Research 3(10), 974–982.

Jay, V., Shafkat, R., 2018: Synthesis of selenium nanoparticles using *Allium sativum* extract and analysis of their antimicrobial property against gram-positive bacteria. The Pharma Innovation 7(9), 262–266.

Khan, Z., Al-Thabaiti, S.A., Hussain, S., 2016: Nanoscale water-soluble self-assembled zero-valent iron: role of stabilizers in their morphology. RSC Advances 6(9), 7267–7278.

Kianpour, S., Ebrahiminezhad, A., Mohkam, M., Tamaddon, A.M., Dehshahri, A., Heidari, R., 2017: Physicochemical and biological characteristics of the nanostructured polysaccharide- iron hydrogel produced by microorganism *Klebsiella oxytoca*. Journal of Basic Microbiology 57(2), 132–140.

Kim, J.S., Kuk, E., Yu, K.N., Kim, J.H., Park, S.J., Lee, H.J., Kim, S.H., Park, Y.K., Park, Y.H., Huwang, Y., Kim, Y.K., Lee, Y.S., Jeong, D.H., Cho, M.H., 2007: Antimicrobial effects of silver nanoparticles. Nanomedicine: Nanotechnology, Biology, and Medicine 3(1), 95–101.

Kouhbanani, M.A.J., Beheshtkhoo, N., Amani, A.M., Taghizadeh, S., Beigi, V., Bazmandeh, A.Z., Khalaf, N., 2018: Green synthesis of iron oxide nanoparticles using *Artemisia vulgaris* leaf extract and their application as a heterogeneous Fenton-like catalyst for the degradation of methyl orange. Materials Research Express 5(11), 115013.

Kouhbanani, M.A.J., Beheshtkhoo, N., Taghizadeh, S., Amani, A.M., Alimardani, V., 2019: One-step green synthesis and characterization of iron oxide nanoparticles using aqueous leaf extract of *Teucrium polium* and their catalytic application in dye degradation. Advances in Natural Sciences: Nanoscience and Nanotechnology 10, 015007.

Kulisic, T., Radonic, A., Milos, M., 2005: Antioxidant properties of Thyme (*Thymus vulgaris* L.) and wild thyme (*Thymus serpyllum* L.) essential oils. Italian Journal of Food Science 3(17), 1–10.

Kulkarni, S., Jadhav, M., Raikar, P., Barretto, D.A., Vootla, S.K., Raikar, U.S., 2017: Green synthesized multifunctional Ag@

Fe_2O_3 nanocomposites for effective antibacterial, antifungal and anticancer properties. New Journal of Chemistry 41(17), 9513–9520.

Kumar, B., Smita, K., Cumbal, L., Debut, A., Galeas, S., Guerrero, V.H., 2016: Photosynthesis and photocatalytic activity of magnetic (Fe_3O_4) nanoparticles using the *Andean blackberry* leaf. Materials Chemistry and Physics 179, 310–315.

Kumar, B., Smita, K., Cumbal, L., Debut, A., 2014: Biogenic synthesis of iron oxide nanoparticles for 2-arylbenzimidazole fabrication. Journal of Saudi Chemical Society 18, 364–369.

Latha, N., Gowri, M., 2014: Biosynthesis and characterisation of Fe_3O_4 nanoparticles using *Caricaya Papaya* Leaves Extract. International Journal of Science and Research 3(11), 1551–1556.

Lee, C., Kim, J.Y., Lee, W.I., Nelson, K.L., Yoon, J., Sedlak, D.L., 2008: Bactericidal effect of zero-valent iron nanoparticles on *Escherichia coli*. Environmental Science and Technology 42(13), 4927–4933.

Luo, F., Chen, Z., Megharaj, M., Naidu, R., 2014: Biomolecules in grape leaf extract involved in one-step synthesis of iron-based nanoparticles. RSC Advances 4, 53467–53474.

Madivoli, E.S., Kareru, P.G., Maina, E.G., Nyabola, A.O., Wanakai, S.I., Nyang`au, J.O., 2019: Biosynthesis of iron nanoparticles using *Ageratum conyzoides* extracts, their antimicrobial and photocatalytic activity. SN Applied Science 1, 500.

Madhavi, V., Prasad, T.N.V.K.V., Reddy, V.B, Ravindra, R.B., Madhavi, G., 2013: Application of phytogenic zerovalent iron nanoparticles in the adsorption of hexavalent chromium. Spectrochimica Acta A: Molecular and Biomolecular Spectroscopy 116, 17–25.

Makarov, V.V., Makarova, S.S., Love, A.J., Sinitsyna, O.V., Dudnik, A.O., Yaminsky, I.V., Taliansky, M.E., Kalinina, N.O., 2014: Decolorization of reactive dyes in solar pond reactors: Perspectives and challenges for the textile industry. Langmuir 30, 5982.

Mandal, D., Bolander, M.E., Mukhopadhyay, D., Sarkar, G., Mukherjee, P., 2006: The use of microorganisms for the formation of metal nanoparticles and their application. Applied Microbiology and Biotechnology 69, 485–492.

Mehdi, F., Kourosh, R., Ahmad, Z., Hossein, A., Fakhraddin, N., Rasoul, K., 2017: A novel green synthesis of zero valent iron nanoparticles (NZVI) using three plant extracts and their efficient application for removal of Cr(VI) from aqueous solutions. Advanced Powder Technology 28, 122–130.

Moraru, C.I., Panchapakesan, C.P., Huang, Q., Takhistove, P., Liu, S., Kokini, J.L., 2003: Nanotechnology: a new frontier in food science. Food Technology 57(12), 24–29.

Nasrollahzadeh, M., Mohammad, S.S., Akbar, R.V., Sarbast, M.H., 2016: Green synthesis of CuO nanoparticles using aqueous extract of *Thymus vulgaris* L. leaves and their catalytic performance for N-arylation of indoles and amines. Journal of Colloid and Interface Science 466, 113–119.

Niraimathee, V., Subha, V., Ravindran, R.E., Renganathan, S., 2016: Green synthesis of iron oxide nanoparticles from *Mimosa pudica* root extract. International Journal of Environment and Sustainable Development 15(3), 227–240.

Njagi, E.C., Huang, H., Stafford, L., Genuino, H., Galindo, H.M., Collins, J.B., Hoag, G.E., Suib, S.L., 2011: Biosynthesis of iron and silver nanoparticles at room temperature using aqueous *Sorghum bran* extracts. Langmuir 27, 264–271.

Pattanayak, M., Nayak, P.L., 2013: Eco-friendly green synthesis of iron nanoparticles from various plants and spices extract. International Journal of Plant, Animal and Environmental Sciences 3(1), 68–76.

Saraniya, J.D., Bhimba, V., 2014: Antibacterial and antifungal activity of silver nanoparticles synthesized using *Hypnea muciformis*. Bioscience Biotechnology Research Asia 11(1), 235–238.

Saif, S., Tahir, A., Chen, Y., 2016: Green synthesis of iron nanoparticles and their environmental applications and implications. Nanomaterials 6, 209.

Seddighi, N.S., Salari, S., Izadi, A.R., 2017: Evaluation of antifungal effect of iron-oxide nanoparticles against different *Candida* species. IET Nanobiotech 11(7), 883–888.

Shah, M., Derek, F., Shashi, S., Suraj, K.T., Gérrard, E.J.P., 2015: Green synthesis of metallic nanoparticles via biological entities. Materials 8, 7278–7308.

Siddiqi, K.S., Husen, A., Rao, R.A., 2018: A review on biosynthesis of silver nanoparticles and their biocidal properties. Journal of Nanobiotechnology 16, 14–42.

Singh, J., Dutta, T., Kim, K.H., Rawat, M., Samddar, P., Kumar, P., 2018: Green synthesis of metals and their oxide nanoparticles: application for environmental remediation. Journal of Nanobiotechnology 16(1), 84.

Takeuchi, H., Lu, Z.G., Yu, O., 2007: Distinct crucial roles of flavonoids during legume nodulation. Trends in Plant Science 12(7), 282–285.

Trotte, N.S.F., Aben-Athar, M.T.G., Carvalho, N.M.F., 2016: Yerba mate tea extract: a green approach for the synthesis of silica supported iron nanoparticles for dye degradation. Journal of the Brazilian Chemical Society 27, 2093–2104.

Violeta, V., Catalin, P., Constantin, F., Monica, A., Marius, B., 2011: Nanoparticles applications for improving the food safety and food processing conference. In: Visa, I. (ed.), The 7th International Conference on Materials Science and Engineering, 24–77. Faculty of Materials Science and Engineering, Transilvania University of Brasov, Romanian Technical Sciences Academy, Bramat, Brasov.

Wang, Z., Fang, C., Mallavarapu, M., 2015: Characterization of iron–polyphenol complex nanoparticles synthesized by sage (*Salvia officinalis*) leaves. Environmental Technology and Innovation 4, 92–97.

Wang, Z., Fang, C., Megharaj, M., 2014: Characterization of iron–polyphenol nanoparticles synthesized by three plant extracts and their fenton oxidation of azo dye. ACS Sustainable Chemistry and Engineering 2(4), 1022–1025.

Yehia, R.S., Al-Sheikh, H., 2014: Biosynthesis and characterization of silver nanoparticles produced by *Pleurotus ostreatus* and their anticandidal and anticancer activities. World Journal of Microbiology and Biotechnology 30, 2797–2830.

Zhao, X., Liu, W., Cai, Z., Han, B., Qian, T., Zhao, D., 2016: An overview of preparation and applications of stabilized zerovalent iron nanoparticles for soil and ground water remediation. Water Research 100, 245–266.